Eur. Phys. J. C (2009) 61: 357–367
DOI 10.1140/epjc/s10052-009-1010-6

THE EUROPEAN PHYSICAL JOURNAL C

Regular Article - Theoretical Physics

# Duality between different mechanisms of QCD factorization in $\gamma^*\gamma$ collisions

**I.V. Anikin**[1,a], **I.O. Cherednikov**[1,2,3,b], **N.G. Stefanis**[2,c], **O.V. Teryaev**[1,d]

[1] Bogoliubov Laboratory of Theoretical Physics, JINR, 141980 Dubna, Russia
[2] Institut für Theoretische Physik II, Ruhr-Universität Bochum, 44780 Bochum, Germany
[3] INFN Gruppo collegato di Cosenza, 87036 Rende, Italy

Received: 19 December 2008 / Revised: 3 February 2009 / Published online: 8 April 2009


**Abstract** We study the phenomenon of duality in hard exclusive reactions to which QCD factorization applies. Considering "two-photon"-like processes in the scalar $\varphi^3_E$ model and also two-hadron (pion) production from the collisions of a real (transversely polarized) and a highly-virtual, longitudinally polarized photon in QCD, we identify two regimes of factorization, each of them associated with a distinct nonperturbative mechanism. One mechanism involves twist-3 Generalized Distribution Amplitudes, whereas the other one employs leading-twist Transition Distribution Amplitudes. In the case of the scalar $\varphi^3_E$ model, we find duality in that kinematical region where the two mechanisms overlap. In the QCD case, the appearance of duality is sensitive to the particular nonperturbative model applied and can, therefore, be used as an additional adjudicator.

**PACS** 13.40.-f · 12.38.Bx · 12.38.Lg

## 1 Introduction

Lacking a complete theoretical understanding of color confinement, the only method of applying QCD is based on the factorization of the dynamics and the isolation of a short-distance part which is amenable to perturbative techniques of quantum field theory (see, [1–5] and for a review, for instance, [6] and references cited therein). On the other hand, the long-distance part has to be parameterized in terms of matrix elements of quark and gluon operators between hadronic states (or the vacuum). These matrix elements have a nonperturbative origin and have to be either extracted from experiment or be determined by lattice simulations. In many phenomenological applications they are usually modeled by applying various nonperturbative methods.

The QCD description of more involved hadronic processes requires the introduction of new hard parton subprocesses and nonperturbative functions. Important particular examples are exclusive hadronic processes which involve hadron distribution amplitudes (DAs), generalized distribution amplitudes (GDAs), and generalized parton distributions (GPDs) [7–11]. Within this context, collisions of a real and a highly-virtual photon provide a useful tool for studying a variety of fundamental aspects of QCD. A special case of this large class of processes is the exclusive two-hadron (pion) production in that region, where one initial photon is far off-shell (with its virtuality being denoted by $Q^2$) and longitudinally polarized, with the other photon being transversely polarized, while the overall energy (or, equivalently, the invariant mass of the two hadrons), $s$, is small. Such a process factorizes into a perturbatively calculable short-distance dominated subprocess, that describes the scattering $\gamma^*\gamma \to q\bar{q}$ or $\gamma^*\gamma \to gg$, and nonperturbative matrix elements measuring the transitions $q\bar{q} \to AB$ and $gg \to AB$.

Another extensively studied—both theoretically and experimentally—two-photon process is the pion–photon transition form factor. This exclusive process has been measured by the CELLO [12] and the CLEO [13] Collaborations for an almost on-shell (i.e., real) photon, whereas the other one has a large virtuality of up to 9 GeV$^2$ and is transversely polarized. These data have been analyzed over the years by many authors using various theoretical approaches—see, for instance, [14–23]. The major outcome of the most recent study [22] is that the CLEO data exclude the Chernyak–Zhitnitsky pion distribution amplitude [24] at the $4\sigma$ level, while, perhaps somewhat surprisingly, also the asymptotic distribution amplitude seems to be disfavored (being off at the $3\sigma$ level). These findings are supported by the latest

[a] e-mail: anikin@theor.jinr.ru
[b] e-mail: igor.cherednikov@jinr.ru
[c] e-mail: stefanis@tp2.ruhr-uni-bochum.de
[d] e-mail: teryaev@theor.jinr.ru

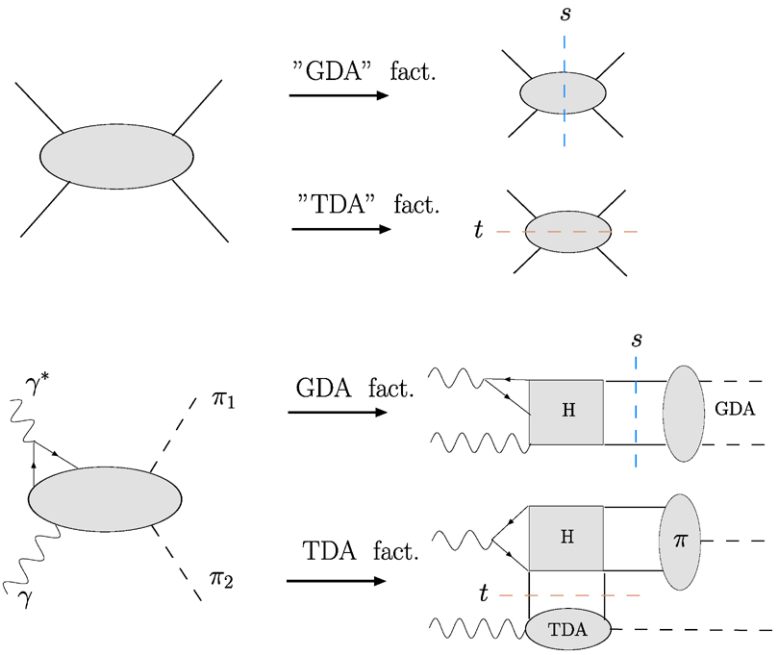


**Fig. 1** (*Top*) Dual factorization mechanisms in describing the fusion of a real photon with a highly-virtual and longitudinally polarized photon in the Euclidean $\varphi^3_E$ model. (*Bottom*) The analogous situation in QCD

high-precision lattice simulations by two independent collaborations [25, 26]. It is remarkable that the only pion distribution amplitude found to be within the $1\sigma$ error ellipse of the CLEO data, while complying with the new lattice results just mentioned, is the pion model derived from nonlocal QCD sum rules [27].

These results lend credibility to the usefulness of two-photon processes as a means of accessing and understanding the parton structure of hadrons. On that basis, one may try to assess more complicated two-photon processes with two pions in the final state. Indeed, recently, nonperturbative quantities of a new kind were introduced—transition distribution amplitudes (TDAs) [28–30]—which are closely related to the GPDs and describe the transition $q\gamma \to qA$. In contrast to the GDAs, mentioned above, such nonperturbative objects, like the TDAs, appear in the factorization procedure when the Mandelstam variable $s$ is of the same order of magnitude as the large photon virtuality $Q^2$, while $t$ is rather small. Actually, there exists a reaction where both amplitude types, GDAs and TDAs, can overlap. Precisely this can happen in the fusion of a real transversely polarized photon with a highly-virtual longitudinally polarized photon that gives rise to a final state comprising a pair of pions. This reaction can potentially follow either path, i.e., it can proceed via the twist-3 GDAs, or through the leading-twist TDAs, as illustrated in Fig. 1. The first mentioned possibility is linked to the case when one of the involved photons is longitudinally polarized, whereas the other one is transversely polarized. The second possibility corresponds to the same situation, but appears in contrast to that in leading-twist order, as we will show in Sect. 3. Thus, a comparative analysis of both possible mechanisms for this reaction seems extremely interesting both theoretically and phenomenologically.

A simultaneous analysis of these two mechanisms in the production of a vector-meson pair was carried out in [31]. The authors found that these mechanisms can be selected by means of the different polarizations of the initial-state photon. In the case of (pseudo)scalar particles, like the pions, this effect is absent and, therefore, this opens up a window of opportunity to access the overlap region of both mechanisms and their duality as opposed to their additivity. By duality we mean here that adding the contributions of the two mechanisms would lead to a double counting. Hence, these mechanisms are in antagonism to each other and should be considered as two alternative ways to describe the same physics.

In this paper, we will verify the possibility for duality between the two different mechanisms of factorization, associated either with GDAs, or with TDAs, in the regime where *both* Mandelstam variables $s$ and $t$ are rather small compared to the large photon virtuality $Q^2$. This will be done below by considering first (Sect. 2) the Euclidean $\varphi^3_E$-analogue of QCD, followed by an investigation of the exclusive pion-pair production in $\gamma\gamma^*_L$ collisions in Sect. 3. Our findings are summarized and further discussed in Sect. 4, where we also provide our conclusions.

## 2 Regimes of factorization within the $\varphi^3_E$ model

We start our analysis with the factorization of a two-photon process in which the two photons undergo a fusion with the subsequent creation of two pions. For the sake of simplicity, we work first in the scalar Euclidean $\varphi^3_E$ model, regarding it

as a sort of a toy model in order to prepare the ground for the real QCD application to follow in the subsequent section.

The most convenient way to analyze this four-particle amplitude in the $\varphi_E^3$ model is to work within the $\alpha$-representation, following the lines of thought given in [10] in the discussion of Deeply Virtual Compton Scattering. The reason is that within this representation (i) the calculations can be performed in a systematic way, not only at one loop but also at higher-loop levels, (ii) the factorization of the process can be studied in detail, and (iii) one can study the spectral properties of the nonperturbative input (GPDs, GDAs) because these properties are insensitive to the numerators of the quark and gluon propagators. In addition, complications owing to the spin structure do not affect them. It is worth recalling in this context that the $\alpha$-representation of Feynman diagrams is not only a schematic means for identifying relevant integration regions in a factorization procedure, but can, in fact, serve to provide rigorous proofs of factorization theorems [1, 2].

The contribution of the leading "box" diagram, see Fig. 2, can be written as

$$\mathcal{A}\big(s,t,m^2\big) = -\frac{g^4}{16\pi^2}\int_0^\infty \frac{\prod_{i=1}^4 d\alpha_i}{D^2} \times \exp\Big[-\frac{1}{D}\big(Q^2\alpha_1\alpha_2 + s\alpha_2\alpha_4 + t\alpha_1\alpha_3 + m^2D^2\big)\Big], \tag{1}$$

where $m^2$ serves as a infrared (IR) regulator, $s>0$, $t>0$ are the Mandelstam variables in the Euclidean region, and $D=\alpha_1+\cdots+\alpha_4$.

It is useful to introduce the dimensionless parameters

$$\alpha_i = \frac{\tilde\alpha_i}{\Lambda^2} \tag{2}$$

(here, the dimensional parameter $\Lambda^2$ is an arbitrary one) and, then, recast the $\tilde\alpha$-parameters into the form

$$\tilde\alpha_i\big|_0^\infty = \frac{\beta_i}{1-\beta_i}\bigg|_0^1. \tag{3}$$

As a result, we get the following expression for the considered amplitude:

$$\mathcal{A}\big(s,t,m^2\big) = -\frac{g^4}{16\pi^2\Lambda^4}\,\tilde{\mathcal{A}},$$
$$\tilde{\mathcal{A}} = \int_0^1 \frac{\prod_{i=1}^4 d\beta_i}{\tilde D^2}\exp\Big[-\frac{Q^2}{\Lambda^2}\frac{\beta_1\beta_2\bar\beta_3\bar\beta_4}{\tilde D} - \frac{s}{\Lambda^2}\frac{\beta_2\beta_4\bar\beta_1\bar\beta_3}{\tilde D} - \frac{t}{\Lambda^2}\frac{\beta_1\beta_3\bar\beta_2\bar\beta_4}{\tilde D} - \frac{m^2}{\Lambda^2}\frac{\tilde D}{\bar\beta_1\bar\beta_2\bar\beta_3\bar\beta_4}\Big], \tag{4}$$

where $\tilde D = \beta_1\bar\beta_2\bar\beta_3\bar\beta_4 + \cdots + \bar\beta_1\bar\beta_2\bar\beta_3\beta_4$ and $\bar\beta_i = 1-\beta_i$. The particular feature of the considered process is that the transferred momentum $q^2=Q^2$ is large compared to the mass scale $m^2$, the latter simulating here the typical scale of soft interactions. With respect to the other two kinematical variables $s$ and $t$, one can identify four distinct regimes:

(a) $s \ll Q^2$ while $t$ is of order $Q^2$;
(b) $t \ll Q^2$ while $s$ is of order $Q^2$;
(c) $s,\ t \ll Q^2$;
(d) $s,\ t$ are both of order $Q^2$ (this regime corresponds to large-angle scattering [3, 4] and will not be addressed here).

Notice that within the regimes (a) and (b), amplitude (1) or (4) can be factorized. Recall that the factorization of (1) and (4) at the leading-twist level in the $\alpha$- or $\beta$-representation is equivalent to the calculation of the leading $Q^2$-asymptotics of the Laplace-type integral

$$F(\lambda) = \int_0^\infty d\alpha\, g(\alpha)\exp\big[-\lambda f(\alpha)\big] \approx \frac{g(0)}{\lambda f'(0)}$$

with a large and positive parameter $\lambda$ and the function $f(\alpha)$ having a minimum at the point $\alpha=0$.

*Regime (a)* Let us begin the discussion of this regime by considering how the integrand in (4) depends on the parameters $\beta_1$ and $\beta_2$, keeping in mind that the parameters $\beta_3$ and $\beta_4$ will be integrated out. To model this regime, we fix, for example, the value of $s/\Lambda^2$ to be equal to 1 and set $t/\Lambda^2=50.0$, $Q^2/\Lambda^2=100.0$. Then, the two-variable function representing the integrand in (4) behaves as shown in Fig. 3. From this figure, one can conclude that the main

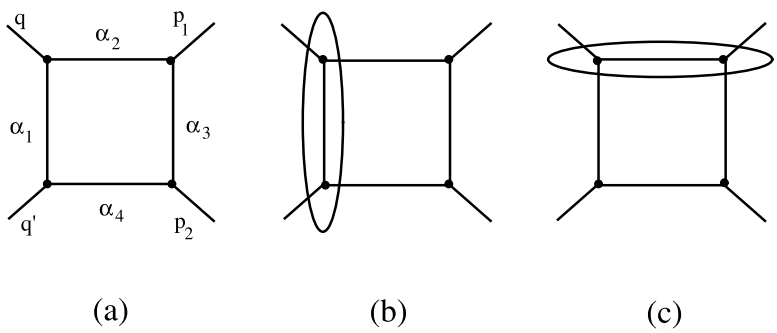


**Fig. 2** (**a**) The box diagram in $\alpha$-space within the $\varphi_E^3$-theory. The *left open lines* in each graph simulate the "photons" with the appropriate kinematics (see text), whereas the *open lines at the right* denote the produced mock "pions". (**b**) "GDA factorization" indicated by an *oval*. (**c**) "TDA factorization" indicated by an *oval*

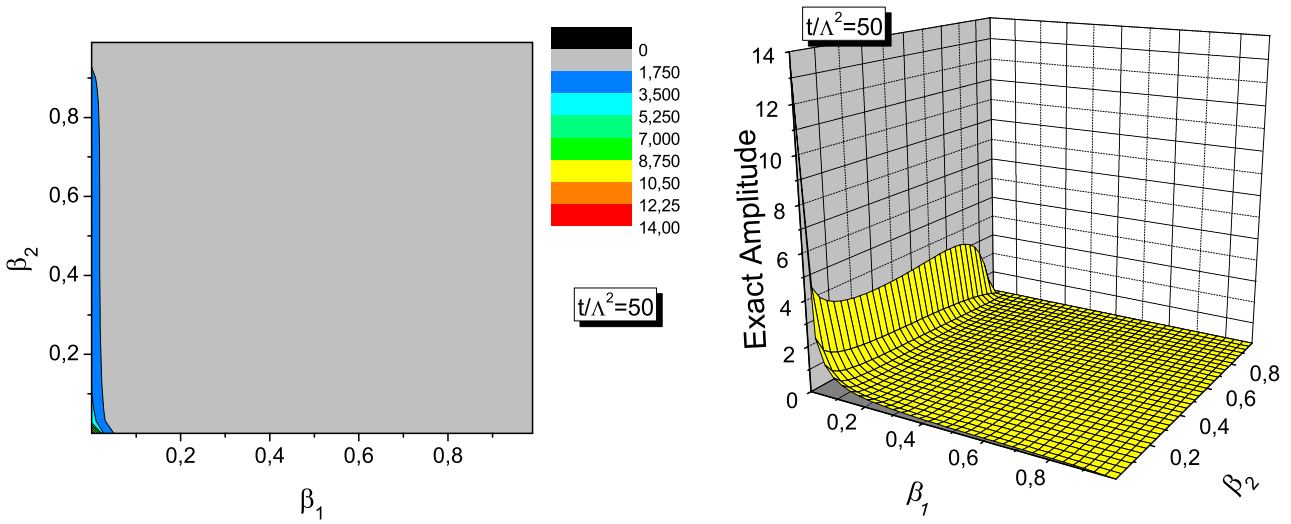


**Fig. 3** The integrand of the exact amplitude (4) as a function of $\beta_1$ and $\beta_2$ in regime (a). *Left panel*: top view; *right panel*: 3D illustration

contribution to the exact amplitude (4) emanates from the area restricted by small $\beta_1$ values around $\beta_1 \sim 0.05$ and $\beta_2$ values varying in the wide interval $[0, 0.9]$. We will call this support of the integrand the $\beta_2$-wing. Indeed, we may divide the whole support into the following domains (see Fig. 4)

$$\begin{aligned}
&\text{Region 1:} \quad \beta_1 \in [0, 0.1], \qquad \beta_2 \in [0, 0.1];\\
&\text{Region 2:} \quad \beta_1 \in [0.1, 1], \qquad \beta_2 \in [0.1, 1];\\
&\text{Region 3:} \quad \beta_1 \in [0, 0.1], \qquad \beta_2 \in [0.1, 1];\\
&\text{Region 4:} \quad \beta_1 \in [0.1, 1], \qquad \beta_2 \in [0, 0.1].
\end{aligned} \tag{5}$$

Our numerical computation shows that the integrations over the strip including the regions 1 and 3 (the $\beta_2$-wing) gives a 85% contribution to the amplitude (4) relative to the contribution from the whole support. Thus, we may approximate the exact amplitude by integrating over the $\beta_2$-wing only. [Note that the contribution from the integration over the region 1 provides approximately a mere 5%.]

On the other hand, in this regime, the exact amplitude can also be estimated by the asymptotic formula which results from the analytic integration over the region where $\beta_1 \sim 0$ (corresponding to the "GDA factorization"—recall Fig. 1):

$$\begin{aligned}
&\tilde{\mathcal{A}}^{\text{as}}_{\text{GDA}}(s,t,m^2)\\
&\quad = \int_0^1 \frac{d\beta_2\, d\beta_3\, d\beta_4}{\tilde{D}_0^2}\\
&\qquad \times \exp\left(-\frac{s}{\Lambda^2}\frac{\beta_2\beta_4\bar{\beta}_3}{\tilde{D}_0} - \frac{m^2}{\Lambda^2}\frac{\tilde{D}_0}{\bar{\beta}_2\bar{\beta}_3\bar{\beta}_4}\right)\\
&\qquad \times \left[\frac{Q^2}{\Lambda^2}\frac{\beta_2\bar{\beta}_3\bar{\beta}_4}{\tilde{D}_0} + \frac{t}{\Lambda^2}\frac{\beta_3\bar{\beta}_2\bar{\beta}_4}{\tilde{D}_0} + \frac{m^2}{\Lambda^2}\right]^{-1},
\end{aligned} \tag{6}$$

**Fig. 4** Regions of integration in $\beta$ space of the integrand of the exact amplitude (4) as a function of $\beta_1$ and $\beta_2$

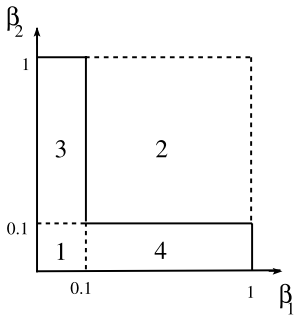


where $\tilde{D}_0 = \beta_2\bar{\beta}_3\bar{\beta}_4 + \bar{\beta}_2\beta_3\bar{\beta}_4 + \bar{\beta}_2\bar{\beta}_3\beta_4$. Indeed, the integration over $\beta_1 \sim 0$ eliminates the $Q^2$-dependence in the exponential function and provides the main contribution to the amplitude $\tilde{\mathcal{A}}$. Schematically, this means that the propagator parameterized by $\alpha_1$ or $\beta_1$ can be associated with the partonic (hard) subprocesses, while the remaining propagator constitutes the soft part of the considered amplitude, i.e., the scalar version of the GDA (see Fig. 2(b)). Note that the considered process is going through the s-channel, which would correspond to the GDA mechanism in QCD.[1]

Concluding this discussion, one should stress that when $s/\Lambda^2 = 1.0$, $t/\Lambda^2 = 50.0$, the ratio between the asymptotic (6) and the exact amplitude (4) is

$$R = \frac{\tilde{\mathcal{A}}^{\text{as}}_{\text{GDA}}}{\tilde{\mathcal{A}}} = 1.01. \tag{7}$$

This ratio shows that the asymptotic formula (6) reproduces the exact amplitude (4) with a rather high accuracy, though slightly overestimating it. Such a situation is very natural for

[1] In anticipation of the QCD case later on, we already use the notions GDA and TDA, though, strictly speaking, they are not applicable here.

the considered regime of the amplitude within the $\alpha$ parameterization and is not at odds with other factorization procedures.

*Regime (b)* Here, we have to eliminate from the exponential in (4) the variables $Q^2$ and $s$, which are large. This can be achieved by integrating over the region $\beta_2 \sim 0$, i.e., by cutting the line corresponding to this parameter. Performing similar manipulations as in regime (a), we find that the scalar TDA amplitude (associated with the factorization in the $t$-channel (see Fig. 2(c))) can be related to the scalar GDA via

$$\tilde{\mathcal{A}}^{\text{as}}_{\text{TDA}}(s,t,m^2) = \tilde{\mathcal{A}}^{\text{as}}_{\text{GDA}}(t,s,m^2). \tag{8}$$

*Regime (c)* The most important regime for our investigations on duality is when it happens that both variables $s$ and $t$ are simultaneously small compared to $Q^2$ (but still much larger than the soft scale $m^2$): $s, t \ll Q^2$. The question which may arise in this case is what happens with factorization. In other words, can the asymptotic formula be useful even in this case?

In investigating this issue, we face two different options.

*Option 1* Start with, say, the regime (a), since there is no doubt that the asymptotic formula (or the factorization) can be applied to both regimes (a) and (b). We begin by considering the integrand of (4) in terms of the two variables $\beta_1$ and $\beta_2$. Then, we tune the value of the variable $t/\Lambda^2$ down to small enough values in order to understand the behavior of the integrand in this regime. We originally designed the integrand of (4) for $t/\Lambda^2$ assuming values within the set $\{25, 10, 5, 2, 1\}$, but for our purposes it is necessary to study the special case of $t/\Lambda^2 = s/\Lambda^2 = 1$ presented in Fig. 5. From this graphics we see that the support of the considered function contains now two wings from which the function becomes saturated. Note that the $\beta_1$- and $\beta_2$-wings are the same in this case and that both wings are equally essential. The numerical analysis shows that the integration in (4) over the regions 1, 3, and 4 ($\beta_1$- and $\beta_2$-wings), i.e.,

$$\begin{aligned}\tilde{\mathcal{A}} \approx \left\{\int_{\text{Reg.-1}} + \int_{\text{Reg.-3}} + \int_{\text{Reg.-4}}\right\} d\beta_1\, d\beta_2 \int_0^1 \frac{d\beta_3\, d\beta_4}{\tilde{D}^2} \\ \times \exp\left[-\frac{Q^2}{\Lambda^2}\frac{\beta_1\beta_2\bar{\beta}_3\bar{\beta}_4}{\tilde{D}} - \frac{s}{\Lambda^2}\frac{\beta_2\beta_4\bar{\beta}_1\bar{\beta}_3}{\tilde{D}}\right. \\ \left. - \frac{t}{\Lambda^2}\frac{\beta_1\beta_3\bar{\beta}_2\bar{\beta}_4}{\tilde{D}} - \frac{m^2}{\Lambda^2}\frac{\tilde{D}}{\bar{\beta}_1\bar{\beta}_2\bar{\beta}_3\bar{\beta}_4}\right]\end{aligned} \tag{9}$$

provides approximately a 80% contribution to the exact amplitude in this regime. Therefore, the saturation of the exact amplitude (4) in regime (c) results from contributions originating from both wings $\beta_1$ and $\beta_2$. Hence, restricting attention to only one of them is not permissible. In this sense, we deal with a particular case of "additivity" of the two wings.

*Option 2* However, there exists an alternative way to determine the exact amplitude, based on the analytic integration of (4) in $\beta$ space. Namely, we may continue the asymptotic formula (6), obtained within regime (a), to regime (c), where $t/\Lambda^2$ and $s/\Lambda^2$ are the same (or approximately the same). Then, we will observe that the asymptotic formula (6) still describes the amplitude

$$\tilde{\mathcal{A}} \approx \tilde{\mathcal{A}}^{\text{as}}_{\text{GDA}}(s,t,m^2)\big|_{t\to s} \tag{10}$$

with an acceptable accuracy, still slightly overestimating the exact amplitude (4). This becomes evident by analyzing the ratio (7) in terms of $t/\Lambda^2$, as depicted in Fig. 6. One sees that the large $t$-tail of ratio (7) is actually well described by

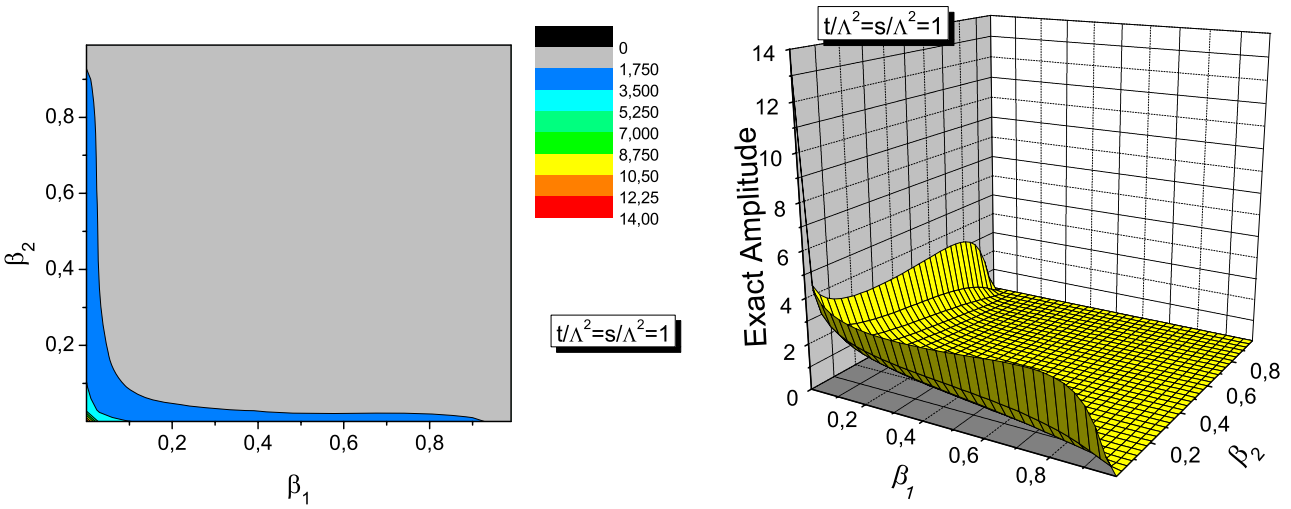


**Fig. 5** The integrand of the exact amplitude (4) as a function of $\beta_1$ and $\beta_2$ in regime (c)

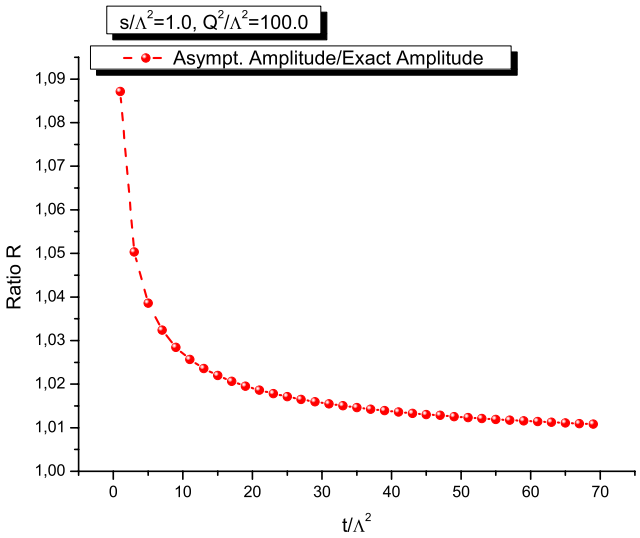


**Fig. 6** The ratio $R$, see (7), as a function of $t/\Lambda^2$

the findings in regime (a). At the same time, when we go to the regime where $t$ is small or of the same order as $s$, the asymptotic formula (6)—which was continued from regime (a)—describes even in this case the exact amplitude with a tolerable 10% deviation. Indeed, in the small $t$ region, the ratio (7) increases from approximately 1.01 to about 1.09 at $t/\Lambda^2 \approx 1$. Hence, we may conclude that, despite the fact that the exact amplitude (4) in regime (c) is saturated from contributions stemming from both wings $\beta_1$ and $\beta_2$, the asymptotic formula (6), derived in regime (a) and continued to regime (c), is still suitable for an acceptable approximation of the exact amplitude.

Due to the symmetry of regimes (a) and (b) under the exchange of the variables $s \leftrightarrow t$, a similar statement is valid as regards the asymptotic formula derived in regime (b)—cf. (8). Therefore, in regime (c), the asymptotic expression (6) still remains a good approximation of the exact amplitude, so that one does not have to re-estimate it using as an alternative equation (8). Insisting to do so, one would face a "double-counting" problem. Thus, in this sense, we deal with duality between (6) and (8). Note that this duality is not a result of the symmetry between regimes (a) and (b). This symmetry merely simplifies the analysis of regime (b).

Since the derivation of the asymptotic formula resembles the factorization procedure for the given amplitude (in which the asymptotic formula plays the role of the partonic part), the GDA and TDA factorizations within the $\varphi_E^3$ model in regime (c) are equivalent to each other without a kinematical or dynamical prevalence of one over the other. This can be interpreted as a sort of duality between the GDA and TDA factorizations.

In concluding this discussion, let us stress that there is a difference between the two possible ways of factorization, which are usually considered to be equivalent, because, there is either dominance of some parts of the full integration region, see (9), or the application of the asymptotic (partonic) formula, see (10) can (approximately) describe the exact process amplitude. In the case of regime (c), the first way of factorization implies additivity of the two wings. Alternatively, the continuation of the asymptotic (partonic) expressions gives rise to duality between them.

## 3 TDA-factorization vs. GDA-factorization for $\gamma\gamma^* \to \pi\pi$

In the preceding section, we demonstrated how the duality between the GDA and the TDA-factorization works within a toy model. We now study the duality phenomenon in the case of real QCD. To this end, we consider the exclusive $\pi^+\pi^-$ production in a $\gamma_T\gamma_L^*$ collision, where the virtual photon with a large virtuality $Q^2$ is longitudinally polarized, whereas the other one is quasi real and transversely polarized. As already mentioned, the key feature of this process is that it exhibits two different kinds of factorization, based, respectively, on the GDA or the TDA mechanism (see Fig. 7), with a potential overlap of both mechanisms in the kinematical regime where $t$ and $s$ are small. Notice that this situation differs from the cases studied in [31], where the additivity of the GDA and the TDA factorizations was explored and found that each factorization mechanism can be selected on account of the helicity of the particles.

In contrast, in our case, the GDA and the TDA regimes correspond to the *same* helicity amplitudes, resembling the situation faced in the scalar case considered in the preceding section where there is only one helicity amplitude. To continue, let us recall the parameterization of nonperturbative matrix elements entering our analysis. Because the considered process involves a longitudinally and a transversally polarized photon, we have to deal with twist-3 parameterizing functions. To this end, we adhere to [32], where the genuine twist-3 contributions in the $\gamma\gamma^* \to \pi\pi$ process were studied in detail (see, also, [33]). As regards the twist-2 contribution, related to the meson DA, we use the standard parameterization of the $\pi^+$-to-vacuum matrix element which involves a bilocal axial-vector quark operator [1, 2].

On the other hand, the $\gamma \to \pi^-$ matrix elements, entering the TDA-factorized amplitude, can be parameterized in the form (cf. [29])

$$\begin{aligned}
&\langle \pi^-(p_2)|\bar\psi(-z/2)\gamma_\alpha[-z/2;z/2]\psi(z/2)|\gamma(q',\varepsilon')\rangle \\
&\quad \stackrel{\mathcal{F}}{=} \frac{ie}{f_\pi}\epsilon_{\alpha\varepsilon'_T P\Delta_T} V_1(x,\xi,t), \\
&\langle \pi^-(p_2)|\bar\psi(-z/2)\gamma_\alpha\gamma_5[-z/2;z/2]\psi(z/2)|\gamma(q',\varepsilon')\rangle \\
&\quad \stackrel{\mathcal{F}}{=} \frac{e}{f_\pi}\varepsilon'_T\cdot\Delta_T P_\alpha A_1(x,\xi,t),
\end{aligned} \tag{11}$$

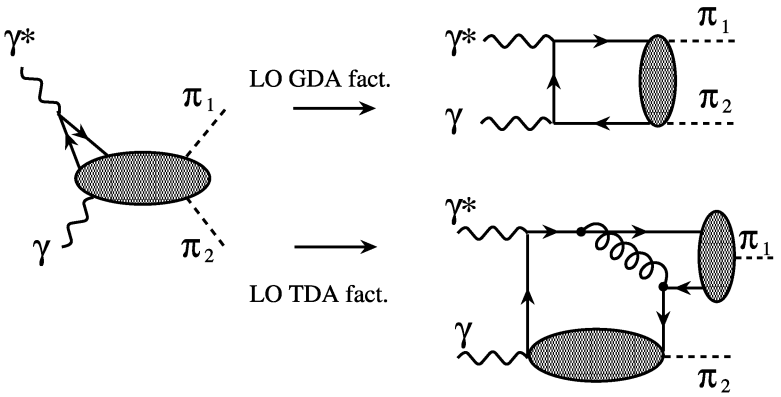


**Fig. 7** Two ways of factorization: (*Left panel*) via the GDA mechanism and via the TDA mechanism (*right panel*). Only a single typical diagram for each case is shown for the purpose of illustration

where the symbol $\stackrel{\mathcal{F}}{=}$ stands for the Fourier transformation (with the appropriate measure) and

$$[-z/2;z/2]=\mathcal{P}\exp\left[ig\int_{z/2}^{-z/2}dx_\mu A_a^\mu(x)t_a\right] \tag{12}$$

denotes a path-ordered gauge link to ensure gauge invariance. In the following, we choose to work in the axial gauge which entails that the gauge link is equal to unity. In (11), the nonperturbative amplitudes $V_1$ and $A_1$ denote, respectively, vector and axial-vector TDAs, whereas the relative momentum is defined as $P=(p_2+q')/2$, and $\Delta=p_2-q'$. Notice that TDAs in the ERBL region, i.e., $-\xi\le x\le\xi$, include the so-called $D$-term, where the pole contribution, related to the spinless resonance (this being the pion in our case), is included [34, 35]. Finally, to normalize the axial-vector TDA, $A_1$, we adopt the philosophy of [29, 36–41] and express $A_1$ in terms of the axial-vector form factor measured in the weak decay $\pi\to l\nu_l\gamma$, i.e.,

$$\int_{-1}^{1}dx\,A_1(x,\xi,t)=2f_\pi F_A(t)/m_\pi, \tag{13}$$

where $f_\pi=0.131$ GeV, $m_\pi=0.140$ GeV, and $F_A(0)\approx 0.012$ [42, 43].

The next objects of interest in our considerations are the helicity amplitudes that are obtained from the usual amplitudes after multiplying them by the photon polarization vectors:

$$\mathcal{A}_{(0,\pm)}=\varepsilon_\mu^{(0)}T^{\mu\nu}_{\gamma\gamma^*}\varepsilon'^{(\pm)}_\nu,\qquad \varepsilon'^{(\pm)}=\left(0,\frac{\mp1}{\sqrt{2}},\frac{+i}{\sqrt{2}},0\right),$$
$$\varepsilon^{(0)}=\left(\frac{|\vec{q}\,|}{\sqrt{q^2}},0,0,\frac{q_0}{\sqrt{q^2}}\right). \tag{14}$$

Discarding the $\Delta_T^2$ corrections, the only remaining contribution stems from the axial-vector one ($A_1$) given by (11). Thus, the helicity amplitude associated with the TDA mechanism reads

$$\mathcal{A}^{\rm TDA}_{(0,j)}=\frac{\varepsilon'^{(j)}\cdot\Delta^T}{|\vec{q}\,|}\mathcal{F}^{\rm TDA},$$
$$\mathcal{F}^{\rm TDA}=\left[4\pi\alpha_s\left(Q^2\right)\right]\frac{C_F}{2N_c}\int_0^1 dy\frac{\phi_\pi(y)}{y\bar{y}}\times\int_{-1}^{1}dx\,A_1(x,\xi,t)\left(\frac{e_u}{\xi-x}-\frac{e_d}{\xi+x}\right), \tag{15}$$

where

$$\xi^{-1}=1+\frac{2W^2}{Q^2}, \tag{16}$$

and where we have employed the one-loop $\alpha_s(Q^2)$ in the $\overline{\rm MS}$-scheme with $\Lambda_{\rm QCD}=0.312$ GeV for $N_f=3$ [44]. We emphasize that the hard part of the amplitude (15), which is factorized at the leading order, contains the QCD coupling constant $\alpha_s$, see Fig. 7. Despite of this, there is only a mild dependence on $\Lambda_{\rm QCD}$. Choosing, for instance, a somewhat smaller value, say, around 0.200 GeV, would shift the TDA curves shown in Fig. 8 slightly downwards.

On the other hand, the helicity amplitude which includes the twist-3 GDA can be written as (see, for example, [32, 33])

$$\mathcal{A}^{\rm GDA}_{(0,j)}=\frac{\varepsilon'^{(j)}\cdot\Delta^T}{|\vec{q}\,|}\mathcal{F}^{\rm GDA},$$
$$\mathcal{F}^{\rm GDA}=\left(e_u^2+e_d^2\right)\frac{W^2+Q^2}{Q^2}\times\int_0^1 dy\,\partial_\zeta\Phi_1\left(y,\zeta,W^2\right)\left(\frac{\ln\bar{y}}{y}-\frac{\ln y}{\bar{y}}\right), \tag{17}$$

where

$$2\zeta-1=\beta\cos\theta^\pi_{cm},\qquad \cos\theta^\pi_{cm}=\frac{2t}{W^2+Q^2}-1 \tag{18}$$

and the partial derivative is defined, as usual, by $\partial_\zeta = \partial/\partial\zeta$. Here the amplitude $\Phi_1(y,\zeta,W^2)$ encodes the matrix element of the twist-2 operator. In deriving (17), we have used the Wandzura–Wilczek approximation for the twist-3 contribution and took into account that in our system $(p_2 - p_1)^T = 2(p_2 - q')^T$.

We would like to stress that the factorized amplitudes (15) and (17) are both of order $1/Q^2$, which offers room for duality. In other words, the necessary condition for observing duality is that the leading asymptotics[2] of the exact amplitudes, corresponding to the TDA- and the GDA-mechanisms—see Fig. 7, must have the same order of $1/Q^2$. Besides, one can infer that the duality between the factorized amplitudes (15) and (17) implies, in a sense, the appearance of duality also between the perturbative and nonperturbative parts of the corresponding factorized amplitudes because the mentioned amplitudes have completely different hard-coefficient functions. Indeed, the hard part of (15) consists of the two (quark and gluon) propagators and includes $\alpha_s$ in contrast to (17), in which the hard-coefficient function is formed only by the quark propagator. Moreover, duality between expressions (15) and (17) may occur in that regime where both Mandelstam variables $s$ and $t$ are much smaller in comparison to the large photon virtuality $Q^2$. In terms of the skewness parameters $\xi$ and $\zeta$, this would imply that $\xi \sim 1$ and $\zeta \sim 0$.

To estimate the relative weight of the amplitudes with TDA or GDA contributions, we have to model these nonperturbative objects.

Let us start with the TDAs. As a first step, we assume a factorizing ansatz for the $t$-dependence of the TDAs and write

$$A_1(x,\xi,t) = 2\frac{f_\pi}{m_\pi} F_A(t) A_1(x,\xi), \tag{19}$$

where the $t$-independent function $A_1(x,\xi)$ is normalized to unity:

$$\int_{-1}^{1} dx\, A_1(x,\xi) = 1. \tag{20}$$

To satisfy this condition, we introduce a TDA defined by

$$A_1(x,1) = \frac{A_1^{\text{non-norm}}(x,1)}{\mathcal{N}}, \quad \mathcal{N} = \int_{-1}^{1} dx\, A_1^{\text{non-norm}}(x,1). \tag{21}$$

We now focus on the discussion of the $t$-independent TDAs in (19). Since we are mainly interested in TDAs in the Efremov–Radyushkin–Brodsky–Lepage (ERBL) [1–4] region $\xi = 1$, it is instructive to choose the following parameterization:

$$A_1^{\text{non-norm}}(x,1) = \big(1-x^2\big)\big(1 + a_1 C_1^{(3/2)}(x) + a_2 C_2^{(3/2)}(x) + a_4 C_4^{(3/2)}(x)\big), \tag{22}$$

where $a_1, a_2, a_4$ are free adjustable parameters, encoding nonperturbative input, and the standard notations for Gegenbauer polynomials are used. One appreciates that the TDA in the form of (22) amounts to summing a $D$-term, i.e., the term with the coefficient $a_1$, and meson-DA-like contributions. Indeed, would we eliminate the term with $a_1$, we would obtain the standard parameterization for a meson DA. On the other hand, keeping only the term with $a_1$, would reproduce the parameterization for the $D$-term [11]. Therefore, for our analysis, we suppose that $a_1 \equiv d_0$ [11], which is equal to $-0.5$ in lattice simulations [45].[3] With respect to the parameters $a_2$ and $a_4$, we allow them to vary in quite broad intervals, notably, $a_2 \in [0.3, 0.6]$ and $a_4 \in [0.4, 0.8]$, that would cover vector-meson DAs with very different profiles at a normalization scale $\mu^2 \sim 1\ \text{GeV}^2$ (see, for example, [47]). Note that the profiles obtained with ansatz (22) bear remarkable resemblance to the TDAs calculated within a non-local chiral quark–soliton model in the recent work of Ref. [36].

As regards the function $\Phi_1(z,\zeta)$, which denotes the corresponding GDA in (17), we take recourse to the following model [7]:

$$\Phi_1\big(z,\zeta,W^2\big) = 9N_f z\bar{z}(2z-1)\big(\tilde{B}_{10}\big(W^2\big)e^{i\delta_0(W^2)} + \tilde{B}_{12}\big(W^2\big)e^{i\delta_2(W^2)} P_2(\cos\theta_\pi)\big), \tag{23}$$

where the phase shift of the $\pi\pi$ scattering is defined by $\delta_0(W_0 = 0.8) \approx \frac{\pi}{2}$ and $\delta_2(W_0 = 0.8) \approx 0.03\pi$ [48, 49]. In (23), the function $\tilde{B}_{10}$ corresponding to $L = 0$ does not contribute to (17) and, therefore, can be discarded. On the other hand, the function $\tilde{B}_{12}$ can be estimated by the method described in [50]. Since $\tilde{B}_{12}$ corresponds to the two-pion state with $L = 2$ and our GDAs probe only the isoscalar channel, we derive for $\tilde{B}_{12}$ at $W^2$ in the region of the $f_2$-meson $[I^G(J^{PC}) = 0^+(2^{++})]$ mass the following expression:

$$\tilde{B}_{12}\big(W^2\big) = \frac{10}{9}\frac{g_{f_2\pi\pi} f_{f_2} M_{f_2}^3 \Gamma_{f_2}}{(M_{f_2}^2 - W^2)^2 + \Gamma_{f_2}^2 M_{f_2}^2}, \tag{24}$$

where $f_{f_2} = 0.056$ GeV, $M_{f_2} = 1.275$ GeV, $\Gamma_{f_2} = 0.185$ GeV, and the decay constant $g_{f_2\pi\pi}$ is defined by

$$g_{f_2\pi\pi} = \sqrt{\frac{24\pi}{M_{f_2}^3}\Gamma(f_2 \to \pi\pi)}, \quad \Gamma(f_2 \to \pi\pi) = 0.85\Gamma_{f_2}. \tag{25}$$

[2] We recall that the factorized amplitude is nothing else than the leading asymptotic form of the exact amplitude in the asymptotic regime $Q^2 \to \infty$.

[3] The case of $a_1 = -4/N_f$, which holds within the chiral quark–soliton model [46], is also included in our analysis. We found that there is no much difference in comparison with the lattice model.

In addition, we also model the function $\tilde{B}_{12}$ with the help of the most simple ansatz (see, [49])

$$\tilde{B}_{12}(0) = \beta^2 \frac{10}{9N_f} R_\pi, \tag{26}$$

where $R_\pi$ denotes the fraction of momentum carried by the quarks and antiquarks in the pion. In our numerical analysis below, we use for this fraction $R_\pi = 0.5$, which is taken from the leading-order Glück–Reya–Schienbein approximation (see, for example, [49]).

Before continuing with the numerical analysis, let us pause for a moment to discuss the validity and self-consistency of the approximations made. Start with the pion DA: for simplicity, the asymptotic pion DA in (15) was used. Using other pion DAs [22], the contribution from the TDA factorization may increase from about 6% for the BMS model [27] to approximately 56% for the CZ model [24]. Second, continue with the GDA: at the level of accuracy relevant for our arguments, we used for the twist-2 GDA $\Phi_1$ the asymptotic form, the justification being provided by quark–hadron duality arguments given in [51]. Third, we assumed the Wandzura–Wilczek approximation, which relies upon the assumption of the smallness of the genuine twist-3 contributions. This assumption is supported by measurements of the $g_2$ structure function. The normalization of the GDA is determined by the momentum conservation which is rigorously valid. By performing a crossing from GPDs (where momentum conservation applies) to the GDA channel, we used the improved expression (24) accounting for meson dynamics. Turn to the TDA: The first ingredient is the normalization (13), which is fixed by the data for the pion weak decay (see for details [29]). Finally, for the form of the TDA, we used a parameterization [cf. (22)], which can accommodate different available models [36–39], within the range of accuracy of the order of 10%, the latter pertaining to our whole numerical analysis.

We calculated both functions $\mathcal{F}^{\rm TDA}$ and $\mathcal{F}^{\rm GDA}$ and show the obtained results in Fig. 8 for $a_1 = -0.5$ (which corresponds to the lattice result of [45]) and employing for simplicity the asymptotic pion DA. The dashed line corresponds to the function $\mathcal{F}^{\rm TDA}$, where we have adjusted the free parameters to $a_2 = 0.6$ and $a_4 = 0.8$. The results, obtained for rather small values of these parameters, are displayed by the broken lines in the same figures. The dotted line denotes the function $\mathcal{F}^{\rm TDA}$ with $a_2 = 0.5$ and $a_4 = 0.6$, whereas the dash-dotted line employs $a_2 = 0.3$ and $a_4 = 0.4$. For comparison, we also include the results for the $\mathcal{F}^{\rm GDA}$. In that latter case, the dense-dotted line corresponds to the GDA amplitude, where the expression for $\tilde{B}_{12}$ has been estimated via (24), while the solid line represents the simplest ansatz (26) with $R_\pi = 0.5$. The particular values of the coefficients $a_2, a_4$, we used, are within the fiducial intervals specified above in conjunction with (22). If, for example, we would have used instead values of these parameters outside their fiducial intervals, then the outcome would change by orders of magnitude and duality would be badly violated.

From this figure one may infer that (i) in the case when the parameter $\tilde{B}_{12}$ (which parameterizes the GDA contribution) is estimated with the aid of the Breit–Wigner formula, see (24), and, while $s, t \ll Q^2$, there is duality between the GDA and the TDA factorization mechanisms. Hence, the model for $\tilde{B}_{12}$ which takes into account the corresponding resonances can be selected by duality. (ii) In the case of the simplest model for $\tilde{B}_{12}$, evaluated for $R_\pi = 0.5$ (see,

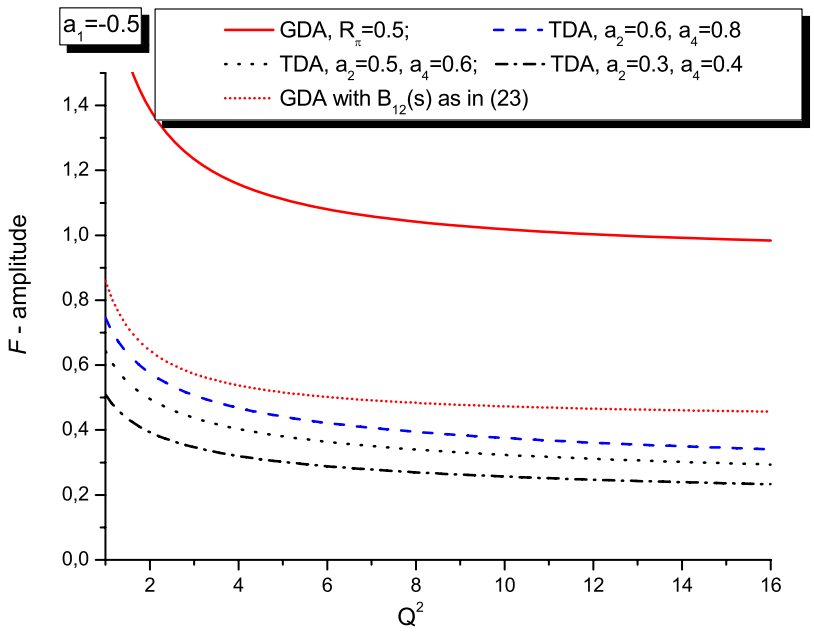


**Fig. 8** Helicity amplitudes $\mathcal{F}^{\rm TDA}$ [cf. (15)] and $\mathcal{F}^{\rm GDA}$ [cf. (17] as functions of $Q^2$, using $a_1 = -0.5$ found in lattice simulations [45] The value of $s/Q^2$ varies in the interval $[0.06, 0.3]$

(26)), the duality between the GDA and the TDA factorization mechanisms reaches maximally the level of 35%, provided the axial-vector TDAs are normalized in terms of the axial form factor $F_A$. On that basis, one may conclude that the simplest model for $\tilde{B}_{12}$ is rather inconsistent with duality and cannot be considered as a realistic option.

## 4 Summary and conclusions

The process amplitude for the fusion of a highly-virtual, but small $s$ photon (longitudinally polarized), with a quasi-real one (with a transversal polarization) can be factorized in two different ways. The study of this process within a toy $\varphi^3_E$ model has shown the existence of duality between the factorization along the $s$-channel and the $t$-channel—which serve to simulate, respectively, the GDA and the TDA factorization mechanisms in QCD. This observation persists also in the case of such reactions in real QCD. Indeed, the amplitude for the process $\gamma\gamma^* \to \pi\pi$ can be factorized in two distinct ways, having recourse to the large virtuality of one of the photons involved, as compared to the scales of the soft interactions. As mentioned before, depending on the variables $s$ and $t$, two different mechanisms for this reaction were identified. The first factorization mechanism, which employs GDAs, takes place when $s \ll Q^2$, while $t$ is of the order of $Q^2$. On the other side, when it happens that $t \ll Q^2$ and $s \sim Q^2$, the TDA mechanism of factorization becomes dominant in such a $\gamma\gamma^*$ collision. We have shown that when both variables $s$ and $t$ are simultaneously much smaller than $Q^2$ in the collision of a real and transversely polarized photon with a highly-virtual longitudinally polarized photon in the pion-pair production, then both types of factorization are possible giving rise to duality in this region.

Our observations in QCD can be summarized and outlined as follows.

We have shown that when it happens that both Mandelstam variables $s$ and $t$ are much less than the large momentum scale $Q^2$, with the variables $s/Q^2$ and $t/Q^2$ varying in the interval $(0.001, 0.7)$, then the TDA and the GDA factorization mechanisms are equivalent to each other and operate in parallel. This marks a crucial difference between our approach and previous ones [31] which dealt with the additivity of the TDA and the GDA factorization mechanisms. Note that the presented results were obtained using rigorous constraints and available nonperturbative models for the DAs, GDAs, and the TDAs. We found that duality appears only for values of the model parameters within their fiducial intervals, associated with each particular model. Therefore, we demonstrated that duality may serve as a tool for selecting suitable models for the nonperturbative ingredients of QCD factorization of various exclusive amplitudes.

In real QCD, we found that duality between the TDA-factorized and GDA-factorized amplitudes can be interpreted as duality between the perturbative and nonperturbative regimes because the hard-coefficient functions of the mentioned amplitudes have completely different structures: the hard part of the TDA-factorized amplitude includes the quark and gluon propagators and the QCD coupling constant, while the hard part of the GDA-factorized amplitude contains only the quark propagator. This situation is not unique in QCD and resembles the so-called quark–hadron duality, which claims that colorless states with given quantum numbers can be described either as a superposition of quark states or alternatively as a superposition of hadron states with the same quantum numbers.

We also observed that twist-3 GDAs appear to be dual to the convolutions of leading-twist TDAs and DAs, multiplied by a QCD effective coupling—the latter stemming from the hard-gluon exchange. This reflects at the level of the particular process, we are considering, the manifestation of duality for the GPDs and GDAs themselves [34, 52, 53]. One may ask to which extent the observed duality between different QCD-factorization mechanisms is an exceptional finding or rather represents a generic feature of QCD dynamics. In this connection, one may recall the different ways of describing single-spin asymmetries (SSA) using either twist-3 collinear factorization [54, 55] or by employing the transverse-momentum dependent (TMD) Sivers distribution function [56]. Because of the T-odd nature of the SSA and the Sivers function, the latter may emerge only due to the interactions between the hard and the soft parts [57] of the process and represents an effective distribution [58]. Moreover, its transverse moment is related [59] to a particular twist-3 matrix element. This sort of relation may be explored [60] as a matching procedure (or, in our language, as duality) between TMD factorization at low $P_T$, on one hand, and collinear twist-3 factorization at large $P_T$, on the other. Recently [61], such a matching procedure was carried out in detail for various observables and it was found that duality strongly depends on the type of the considered observable. In the case of the Sivers function, there is a possibility of enlarging the duality intervals by either using the twist-3 approach at low $P_T$ [62] or by applying the Sivers function at large $P_T$ [63]. The latter procedure finds justification in the framework of the twist-3 factorization, provided only the first non-vanishing transverse moment of the Sivers function is retained and that color factors, responsible for the effective nature of the Sivers function, are properly taken into account.

Duality also emerges when another type of QCD factorization in semi-inclusive processes is considered, which makes use of so-called fracture functions. The momentum conservation guarantees that the description in terms of either fragmentation or fracture functions is complete and one should have duality between these two mechanisms in the overlap region (see [64] and references therein). Bottom

line: We have shown that duality leads to new insights into a number of phenomena in QCD, in particular to those related to exclusive processes and spin-dependent quantities.

**Acknowledgements** We would like to thank A.B. Arbuzov, A.P. Bakulev, A.E. Dorokhov, A.V. Efremov, N. Kivel, B. Pire, M.V. Polyakov, M. Praszałowicz, L. Szymanowski, and S. Wallon for useful discussions and remarks. This investigation was partially supported by the Heisenberg-Landau Programme (Grant 2008), the Deutsche Forschungsgemeinschaft under contract 436RUS113/881/0, the Alexander von Humboldt-Stiftung, the EU-A7 Project *Transversity*, the RFBR (Grants 06-02-16215, 08-02-00896 and 07-02-91557), the Russian Federation Ministry of Education and Science (Grant MIREA 2.2.2.2.6546), the RF Scientific Schools grant 195.2008.9, and INFN.

## References

1. A.V. Efremov, A.V. Radyushkin, Phys. Lett. B **94**, 245 (1980)
2. A.V. Efremov, A.V. Radyushkin, Theor. Math. Phys. **42**, 97 (1980) [Teor. Mat. Fiz. **42**, 147 (1980)]
3. G.P. Lepage, S.J. Brodsky, Phys. Lett. B **87**, 359 (1979)
4. G.P. Lepage, S.J. Brodsky, Phys. Rev. D **22**, 2157 (1980)
5. J.C. Collins, D.E. Soper, G. Sterman, Adv. Ser. High Energy Phys. **5**, 1 (1988). arXiv:hep-ph/0409313
6. N.G. Stefanis, Eur. Phys. J. direct C7, 1 (1999). arXiv:hep-ph/9911375
7. M. Diehl, Phys. Rep. **388**, 41 (2003). arXiv:hep-ph/0307382
8. A.V. Belitsky, A.V. Radyushkin, Phys. Rep. **418**, 1 (2005). arXiv:hep-ph/0504030
9. X.D. Ji, Phys. Rev. D **55**, 7114 (1997). arXiv:hep-ph/9609381
10. A.V. Radyushkin, Phys. Rev. D **56**, 5524 (1997). arXiv:hep-ph/9704207
11. K. Goeke, M.V. Polyakov, M. Vanderhaeghen, Prog. Part. Nucl. Phys. **47**, 401 (2001). arXiv:hep-ph/0106012
12. H.J. Behrend et al., Z. Phys. C **49**, 401 (1991)
13. J. Gronberg et al. (CLEO Collaboration), Phys. Rev. D **57**, 33 (1998). arXiv:hep-ex/9707031
14. P. Kroll, M. Raulfs, Phys. Lett. B **387**, 848 (1996). arXiv:hep-ph/9605264
15. A.V. Radyushkin, R.T. Ruskov, Nucl. Phys. B **481**, 625 (1996). arXiv:hep-ph/9603408
16. N.G. Stefanis, W. Schroers, H.C. Kim, Phys. Lett. B **449**, 299 (1999). arXiv:hep-ph/9807298
17. N.G. Stefanis, W. Schroers, H.C. Kim, Eur. Phys. J. C **18**, 137 (2000). arXiv:hep-ph/0005218
18. A. Schmedding, O.I. Yakovlev, Phys. Rev. D **62**, 116002 (2000). arXiv:hep-ph/9905392
19. M. Diehl, P. Kroll, C. Vogt, Eur. Phys. J. C **22**, 439 (2001). arXiv:hep-ph/0108220
20. A.P. Bakulev, S.V. Mikhailov, N.G. Stefanis, Phys. Rev. D **67**, 074012 (2003). arXiv:hep-ph/0212250
21. A.P. Bakulev, S.V. Mikhailov, N.G. Stefanis, Phys. Lett. B **578**, 91 (2004). arXiv:hep-ph/0303039
22. A.P. Bakulev, S.V. Mikhailov, N.G. Stefanis, Phys. Rev. D **73**, 056002 (2006). arXiv:hep-ph/0512119
23. N.G. Stefanis, Talk given at International Workshop on e+ e− Collisions from Phi to Psi (PHIPSI08), Frascati, Italy, 7–10 Apr. 2008. arXiv:0805.3117 [hep-ph]
24. V.L. Chernyak, A.R. Zhitnitsky, Phys. Rep. **112**, 173 (1984)
25. V.M. Braun et al., Phys. Rev. D **74**, 074501 (2006). arXiv:hep-lat/0606012
26. M.A. Donnellan et al., PoS LATTICE2007, 369 (2006). arXiv:0710.0869 [hep-lat]
27. A.P. Bakulev, S.V. Mikhailov, N.G. Stefanis, Phys. Lett. B **508**, 279 (2001). [Erratum-ibid. B **590**, 309 (2004)]. arXiv:hep-ph/0103119
28. L.L. Frankfurt, M.V. Polyakov, M. Strikman, arXiv:hep-ph/9808449
29. B. Pire, L. Szymanowski, Phys. Rev. D **71**, 111501 (2005). arXiv:hep-ph/0411387
30. J.P. Lansberg, B. Pire, L. Szymanowski, Phys. Rev. D **73**, 074014 (2006). arXiv:hep-ph/0602195
31. B. Pire, M. Segond, L. Szymanowski, S. Wallon, Phys. Lett. B **639**, 642 (2006). arXiv:hep-ph/0605320
32. I.V. Anikin, O.V. Teryaev, Phys. Lett. B **509**, 95 (2001). arXiv:hep-ph/0102209
33. N. Kivel, L. Mankiewicz, Phys. Rev. D **63**, 054017 (2001). arXiv:hep-ph/0010161
34. M.V. Polyakov, Nucl. Phys. B **555**, 231 (1999). arXiv:hep-ph/9809483
35. M.V. Polyakov, C. Weiss, Phys. Rev. D **60**, 114017 (1999). arXiv:hep-ph/9902451
36. P. Kotko, M. Praszałowicz, arXiv:0803.2847 [hep-ph]
37. B.C. Tiburzi, Phys. Rev. D **72**, 094001 (2005). arXiv:hep-ph/0508112
38. W. Broniowski, E.R. Arriola, Phys. Lett. B **649**, 49 (2007). arXiv:hep-ph/0701243
39. A. Courtoy, S. Noguerra, Phys. Rev. D **76**, 094026 (2007). arXiv:0707.3366 [hep-ph]
40. I.V. Anikin, A.E. Dorokhov, L. Tomio, Phys. Part. Nucl. **31**, 509 (2000). [Fiz. Elem. Chast. Atom. Yadra **31**, 1023 (2000)]
41. I.V. Anikin, A.E. Dorokhov, A.E. Maksimov, L. Tomio, V. Vento, Nucl. Phys. A **678**, 175 (2000)
42. W.M. Yao et al. (Particle Data Group), J. Phys. G **33**, 1 (2006)
43. M. Bychkov et al., arXiv:0804.1815 [hep-ex]
44. A.L. Kataev, G. Parente, A.V. Sidorov, Phys. Part. Nucl. **34**, 20 (2003) [Fiz. Elem. Chast. Atom. Yadra **34**, 43 (2003 ERRAT,38,827-827.2007)]. arXiv:hep-ph/0106221
45. M. Göckeler, R. Horsley, D. Pleiter, P.E.L. Rakow, A. Schäfer, G. Schierholz, W. Schroers (QCDSF Collaboration), Phys. Rev. Lett. **92**, 042002 (2004). arXiv:hep-ph/0304249
46. V.Y. Petrov, P.V. Pobylitsa, M.V. Polyakov, I. Börnig, K. Goeke, C. Weiss, Phys. Rev. D **57**, 4325 (1998). arXiv:hep-ph/9710270
47. A.P. Bakulev, S.V. Mikhailov, R. Ruskov, arXiv:hep-ph/0006216
48. M. Diehl, T. Gousset, B. Pire, O. Teryaev, Phys. Rev. Lett. **81**, 1782 (1998). arXiv:hep-ph/9805380
49. M. Diehl, T. Gousset, B. Pire, Phys. Rev. D **62**, 073014 (2000). arXiv:hep-ph/0003233
50. I.V. Anikin, B. Pire, L. Szymanowski, O.V. Teryaev, S. Wallon, Phys. Rev. D **71**, 034021 (2005). arXiv:hep-ph/0411407
51. A.V. Radyushkin, Acta Phys. Polon. B **26**, 2067 (1995). arXiv:hep-ph/9511272
52. M.V. Polyakov, A.G. Shuvaev, arXiv:hep-ph/0207153
53. A.M. Moiseeva, M.V. Polyakov, arXiv:0803.1777 [hep-ph]
54. A.V. Efremov, O.V. Teryaev, Phys. Lett. B **150**, 383 (1985)
55. J.w. Qiu, G. Sterman, Phys. Rev. Lett. **67**, 2264 (1991)
56. D.W. Sivers, Phys. Rev. D **41**, 83 (1990)
57. S.J. Brodsky, D.S. Hwang, I. Schmidt, Phys. Lett. B **530**, 99 (2002). arXiv:hep-ph/0201296
58. D. Boer, P.J. Mulders, O.V. Teryaev, Phys. Rev. D **57**, 3057 (1998). arXiv:hep-ph/9710223
59. D. Boer, P.J. Mulders, F. Pijlman, Nucl. Phys. B **667**, 201 (2003). arXiv:hep-ph/0303034
60. X. Ji, J.W. Qiu, W. Vogelsang, F. Yuan, Phys. Rev. Lett. **97**, 082002 (2006). arXiv:hep-ph/0602239
61. A. Bacchetta, D. Boer, M. Diehl, P.J. Mulders, arXiv:0803.0227 [hep-ph]
62. O.V. Teryaev, in *Proc. of the Int. Workshop on Transverse Polarisation Phenomena in Hard Processes—Transversity 2005*, ed. by V. Barone, P.G. Ratcliffe, Como, Sept. 2005 (World Scientific, Singapore, 2006), p. 276
63. P.G. Ratcliffe, O.V. Teryaev, arXiv:hep-ph/0703293
64. O.V. Teryaev, Phys. Part. Nucl. **35**, S24 (2004)